Translational Oncology
www.transonc.com

Volume 6 Number 2 April 2013 pp. 104–111 104

In Vivo c-Met Pathway Inhibition Depletes Human Glioma Xenografts of Tumor-Propagating Stem-Like Cells[1,2]

Prakash Rath*,[3], Bachchu Lal*,[3], Olutobi Ajala*, Yunqing Li*, Shuli Xia*, Jin Kim† and John Laterra*

*Department of Neurology, The Hugo W. Moser Research Institute at Kennedy Krieger Inc and The Johns Hopkins University School of Medicine, Baltimore, MD; †Galaxy Biotech, LLC, Mountain View, CA

Abstract

Solid malignancies contain sphere-forming stem-like cells that are particularly efficient in propagating tumors. Identifying agents that target these cells will advance the development of more effective therapies. Recent converging evidence shows that c-Met expression marks tumor-initiating stem-like cells and that c-Met signaling drives human glioblastoma multiforme (GBM) cell stemness *in vitro*. However, the degree to which tumor-propagating stem-like cells depend on c-Met signaling in histologically complex cancers remains unknown. We examined the effects of *in vivo* c-Met pathway inhibitor therapy on tumor-propagating stem-like cells in human GBM xenografts. Animals bearing pre-established tumor xenografts expressing activated c-Met were treated with either neutralizing anti–hepatocyte growth factor (HGF) monoclonal antibody L2G7 or with the c-Met kinase inhibitor PF2341066 (Crizotinib). c-Met pathway inhibition inhibited tumor growth, depleted tumors of sphere-forming cells, and inhibited tumor expression of stem cell markers CD133, Sox2, Nanog, and Musashi. Withdrawing c-Met pathway inhibitor therapy resulted in a substantial rebound in stem cell marker expression concurrent with tumor recurrence. Cells derived from xenografts treated with anti-HGF *in vivo* were depleted of tumor-propagating potential as determined by *in vivo* serial dilution tumor-propagating assay. Furthermore, daughter xenografts that did form were 12-fold smaller than controls. These findings show that stem-like tumor-initiating cells are dynamically regulated by c-Met signaling *in vivo* and that c-Met pathway inhibitors can deplete tumors of their tumor-propagating stem-like cells.

Translational Oncology (2013) 6, 104–111

Introduction

Glioblastoma multiforme (GBM) is a nearly universally fatal brain tumor with an associated median survival of approximately 14 months despite aggressive surgical resection, radiation therapy, and chemotherapy. GBM is highly heterogeneous at the histopathologic, cellular, and molecular levels and its cell subpopulations display varying sensitivities to cytotoxic agents and emerging therapies designed to target specific oncogenic pathways. Advances over the past decade have found that GBM contains subpopulations of multipotent stem-like cells characterized by their capacity to grow as nonadherent spheres in defined serum-free medium, differentiate along multiple neural cell lineages, and efficiently propagate tumor xenografts that recapitulate the invasive and histopathologic features of clinical GBM [1]. The tumor-propagating capacity of these stem-like cells along with their relative resistance to DNA-damaging agents predicts that therapies directed against stem-like neoplastic cells will delay tumor relapse and prolong patient survival [2,3]. Multiple autocrine and paracrine signaling pathways and microenvironmental cues have been found to support tumor stem-like cell self-renewal and regulate their transition to more differentiated progenitors [4–6].

Address all correspondence to: John Laterra, MD, PhD, The Kennedy Krieger Institute, 707 N. Broadway, Baltimore, MD 21205. E-mail: laterra@kennedykrieger.org

[1]This research was funded by the National Institutes of Health through grants NS43987 (J.L.), CA129192 (J.L.), and NS073611 (J.L.), by the Maryland Stem Cell Research Fund Fellowship (P.R.), and by the James S. McDonnell Foundation (J.L.). B.L., J.L., and J.K. have financial interests related to the anti-HGF mAb L2G7 used in this research.

[2]This article refers to supplementary material, which is designated by Table W1 and is available online at www.transonc.com.

[3]These authors contributed equally.

Received 16 January 2013; Revised 16 January 2013; Accepted 17 January 2013

DOI 10.1593/tlo.13127

The c-Met receptor tyrosine kinase (RTK) and its ligand hepatocyte growth factor (HGF) are strongly implicated in the malignant progression of many solid neoplasms and expression levels correlate with poor prognosis in multiple malignancies including GBM [7–9]. We and others have reported that inhibitors of c-Met pathway activation inhibit the growth of c-Met$^+$ tumor xenografts by inducing apoptosis and inhibiting tumor cell proliferation and angiogenesis [7,10–12]. Evidence has recently emerged from multiple laboratories showing that c-Met is a marker for stem-like tumor-initiating cell subsets and that c-Met signaling induces stemness in human GBM *in vitro* [13–15]. These findings suggest that c-Met signaling enhances tumor malignancy by preventing differentiation or inducing *de novo* formation of dynamically regulated stem-like cells through reprogramming mechanisms. However, the degree to which tumor-propagating stem-like cells depend on c-Met signaling in histologically complex cancers remains unknown and it has yet to be determined if therapeutic *in vivo* c-Met pathway inhibition can target neoplastic stem-like cell subsets. Determining the effects of c-Met pathway inhibition on cancer stem-like cells *in vivo* will aid the clinical translation of c-Met inhibitors and the development of treatment strategies designed to target cancer stem cells.

This present study examines the effects of *in vivo* therapy with two mechanistically distinct c-Met pathway inhibitors currently in clinical development, neutralizing anti-HGF monoclonal antibody (mAb) L2G7 and the small molecule c-Met kinase inhibitor PF2341066 (Crizotinib), on the stem-like cell phenotype in GBM xenografts. We demonstrate that glioma xenograft growth inhibition in response to c-Met pathway inhibition *in vivo* is accompanied by reductions in the tumor-propagating stem-like phenotype based on molecular marker expression, neurosphere-forming capacity, and the capacity of primary xenograft-derived cells to propagate aggressive intracranial tumors. Our results show for the first time that c-Met pathway inhibitor therapy can deplete tumors of their stem-like tumor-initiating cell subpopulations.

Materials and Methods

Cell Culture

U87 cells were originally obtained from American Type Culture Collection (Manassas, VA) and cultured in Dulbecco's modified eagle's medium supplemented with 10% FBS (Gemini Bio-Products, Sacramento, CA), nonessential amino acids and penicillin and streptomycin (Quality Biological Inc, Gaithersburg, MD). The human GBM xenograft lines, Mayo 39 and Mayo 59, were originally obtained from the Mayo Clinic (Rochester, MN) [16]. Primary human brain neural stem cells were isolated from discarded human abortuses as previously described and kindly provided by Dr Alfredo Quinones (Johns Hopkins School of Medicine) [17]. All cells were grown at 37°C in a humidified incubator with 5% CO_2.

For generating and propagating primary glioma neurospheres, excised subcutaneous tumor xenograft tissue was minced, enzymatically dissociated by trypsinization, and seeded at 4×10^5 cells per 10-cm dish in serum-free neurobasal medium supplemented with epidermal growth factor (EGF) and fibroblast growth factor (FGF) (neurosphere medium) as described [15,18]. Free-floating tumor spheres were passaged by mechanical dissociation through a 1- to 200-μl pipette tip, and passages 5 to 8 were used for experimentation. Neurosphere cells derived from U87 xenografts are referred to as U87-NS cells.

For HGF stimulation studies *in vitro*, neurospheres were dissociated to single-cell suspension, plated at 4×10^5 cells per 10-cm dish, and cultured in EGF/FGF-free medium overnight before the addition of HGF (50 ng/ml final concentration, kindly provided by Genentech, Inc, San Francisco, CA) for 30 minutes. For determining effects of c-Met kinase inhibition *in vitro*, dissociated cells were plated in GBM stem cell medium and PF02341066 (kindly provided by Pfizer, Inc, New York, NY) or buffer only was added daily (150 or 300 nM final concentration) for 7 days before embedding cells in 1% agarose. Neurosphere numbers and diameters were quantified by computer-assisted analyses as previously described [19].

Antibodies

Primary antibodies. Phospho–mitogen-activated protein kinase (MAPK) (rabbit, 1:1000), phospho-AKT (rabbit, 1:1000), total AKT (mouse, 1:1000), Oct4 (rabbit, 1:1000), Sox2 (rabbit, 1:500) were from Cell Signaling Technology (Danvers, MA); CD133 (rabbit, 1:400), Nestin (mouse, 1:1000) and neurofilament medium (NF, rabbit, 1:1000) were from Abcam (Cambridge, MA); Musashi (rabbit, 1:1000), βIII-tubulin (mouse, 1:1000), O1 (mouse, 1:500), and glial fibrillary acidic protein (GFAP) (rabbit, 1:250) were from Millipore (Billerica, MA); total Met (rabbit, 1:500) and phospho-Met Tyr1349 (rabbit, 1:200) were from Santa Cruz Biotechnology (Santa Cruz, CA); Nanog (rabbit, 1:500) was from Kamiya Biomedical Company (Seattle, WA); actin (mouse, 1:15,000; rabbit, 1:25,000) was from Sigma-Aldrich (St Louis, MO); and total MAPK (mouse, 1:1000) was from BD Sciences (Franklin Lakes, NJ).

Secondary antibodies. IR dyes IRDye 800CW (goat anti-mouse, 1:15,000) and IRDye 680CW (goat anti-rabbit, 1:20,000) were from LI-COR Biosciences (Lincoln, NE); AF 488 (goat anti-rabbit, 1:800) and AF 488 (goat anti-mouse, 1:400) were from Invitrogen (Carlsbad, CA); and Cy3 (goat anti-mouse, 1:800) was from Jackson ImmunoResearch Laboratories (West Grove, PA).

Subcutaneous and Intracranial Xenografts

All animal experiments were performed according to Johns Hopkins University Animal Care and Use Committee–approved protocols. Subcutaneous U87 glioma xenografts were generated in 6- to 8-week-old *nu/nu* female mice (National Center Institute) by injecting ~3×10^6 cells in the dorsal flank. Mayo xenograft lines were passaged serially in the flanks of nude mice as previously described [20]. Volumes of subcutaneous xenografts were estimated by measuring the length and width with calipers and calculated with the equation: Volume = (length × width^2)/2 [21]. Intracranial tumor volumes were determined by measuring tumor cross-sectional areas in hematoxylin and eosin (H&E)–stained brain sections by computer-assisted image analysis and then applying the formula Volume = (square root of maximum cross-sectional area)^3 [21].

Anti-HGF mAb (L2G7) or isotype control antibody (5G8) were kindly provided by Galaxy Biotech (Sunnyvale, CA) and administered by intraperitoneal injection (5 or 10 mg/kg) every other day for a total of four injections. Met kinase inhibitor PF2341066 (Pfizer Inc) or solute as control (DMSO) was resuspended in phosphate-buffered saline (PBS) and administered by oral gavage (40 mg/kg) everyday for 7 continuous days.

For the serial dilution tumor-propagating experiments (see Figure 4*A*), animals bearing U87 subcutaneous xenografts were treated

with anti-HGF L2G7 or isotype control 5G8 mAb as described above. Xenografts were removed, minced, and trypsinized to dissociate cells as previously described [20,21]. Cells were then passed through 40-μm mesh filters, washed with PBS, labeled with trypan blue and immediately counted using a TC10 automated cell counter (Bio-Rad, Philadelphia, PA) before intracranial injections. Cells were implanted intracranially using 3×10^2 to 1×10^4 viable cells per animal as indicated. Animals were sacrificed for histopathologic analyses when the corresponding 5G8-treated control groups developed neurological signs indicative of near terminal tumor growth.

Histology, Immunohistochemistry, and Immunofluorescence

Brains were placed in 4% paraformaldehyde for 72-hour fixation, cryoprotected in 30% sucrose, sectioned on a cryostat, and stained with H&E as previously described [21]. Tumor volumes were quantified by computer-assisted image analysis as previously described [21,22]. For immunofluorescence, dissociated neurosphere cells were plated and stained according to a protocol outlined in the Human Neural Stem Cell Characterization Kit (Millipore). Undifferentiated neurosphere cells were embedded and sectioned on a cryostat at 5 μm as previously described [23]. Sections were counterstained with Vectashield (Vector Laboratories, Burlingame, CA) mounting medium containing the nuclear counterstain 4′,6-diamidino-2-phenylindole (DAPI). Nonimmune IgG was used as primary IgG in negative controls.

Immunoblots

Semiquantitative immunoblot analysis was performed according to standard procedures using the specific antibodies shown above, as described previously [21]. Briefly, total protein was extracted from glioma xenografts or cells using RIPA lysis buffer containing protease and phosphatase inhibitors (Calbiochem, Darmstadt, Germany) at 4°C. Tissue protein extracts were also sonicated. Proteins were quantified using Coomassie Protein Assay (Thermo Scientific, Waltham, MA) according to the manufacturer's protocol. Sodium dodecyl sulfate–polyacrylamide gel electrophoresis and transfer to nitrocellulose membranes were performed electrophoretically and membranes were blocked with Odyssey LI-COR Blocking Buffer (LI-COR Biosciences) before antibody incubations. In selected circumstances, membranes were stripped and reprobed with anti–β-actin antibodies as a loading control. Proteins were detected and quantified using the Odyssey Infrared Imager (LI-COR Biosciences).

Quantitative Reverse Transcription–Polymerase Chain Reaction

Total RNA was extracted from tissues and cells with QIAzol reagent and RNeasy Mini Kit according to the manufacturer's protocol (Qiagen, Hilden, Germany). Reverse transcription was performed using MuLV Reverse Transcriptase and Oligo (dT) primers (Applied Biosystems, Grand Island, NY), and quantitative real-time polymerase chain reaction was performed with an Applied Biosystems Prism 7900HT Sequence Detection System and iQ5 System (Bio-Rad). Samples were amplified in triplicate and relative expression of each gene was normalized to 18S RNA and generated in the Bio-Rad iQ5 software. The following primers were used: Nestin: forward, 5-aagacttccctcagctttcag-3′, reverse, 5-agcaaagatccaagacgcc-3′; βIII-tubulin: forward, 5-tttggacatctcttcaggcc-3′, reverse, 5-tttcacactccttccgcac-3′; 18S: forward, 5-acaggattgacagattgatagctc-3′, reverse, 5-caaatcgctccaccaactaagaa-3′.

Forced Differentiation and Neurosphere Assays

U87 cells grown as neurospheres (U87-NS) were cultured in serum-free neurobasal medium containing EGF/FGF (neurosphere medium) as described above. Forced differentiation was performed according to previously published methods [15,24,25]. Briefly, U87-NS cells were dissociated to single-cell suspensions and cultured on Matrigel in neurosphere medium lacking FGF for 2 days and then grown in medium containing 1% FBS without EGF/FGF for 5 days. Forced differentiated cells (referred to as U87-FD) were then processed for immunofluorescence as described above.

To quantify neurosphere formation by cells derived from subcutaneous tumor xenografts, primary xenograft-derived neurospheres were dissociated and plated at 4×10^5 cells per 10-cm dish and allowed to grow in neurosphere medium for 1 week before embedding in 1% agarose for quantification. Neurosphere numbers were counted by computer-assisted image analysis. For HGF stimulation studies *in vitro*, U87-NS cells were dissociated to single-cell suspension, plated at 4×10^5 cells per 10-cm dish, and cultured in neurosphere medium lacking EGF/FGF overnight before the addition of purified recombinant HGF (50 ng/ml, kindly provided by Genentech, Inc) for 30 minutes. For c-Met inhibition conditions, after cell plating, PF02341066 was added daily (150 or 300 nM final concentration) for 7 days before 1% agarose embedding and analysis. Neurospheres greater than 100 μm were quantified and compared to control cells treated with DMSO only.

Results

Systemic Anti-HGF Therapy Depletes HGF-Dependent GBM Xenografts of Stem-Like Cells

We established that U87 xenografts contain sphere-forming multipotent stem-like cells as an initial step toward asking if c-Met activity modulates stem-like GBM cell phenotypes *in vivo*. Single-cell suspensions obtained from U87 xenografts (established by serial subcutaneous passage) and immediately cultured in neurosphere medium readily formed large spheres (referred to as U87-NS cells) demonstrating the presence of stem-like phenotypes in a subset of xenograft cells (Figure 1*A*, U87-NS). These U87-NS cells maintained in neurosphere medium self-renewed under sphere-forming culture conditions for >40 passages and expressed the stem cell molecular markers GFAP, Nestin, Musashi, and Sox2 (Figure 1*B*). U87-NS cells adopted an adherent growth pattern and expressed differentiation molecular markers βIII-tubulin, O1, and intermediate neurofilament, consistent with multilineage neural differentiation potential, in response to forced differentiation induced by growth factor withdrawal and serum (Figure 1*B*).

We evaluated levels of stem cell marker mRNA and protein in U87, U87-NS, and U87-NS cells subjected to forced differentiation (U87-FD). The progenitor cell marker Nestin, which is highly expressed in multipotent human neural stem cells (hNSCs), was expressed minimally in U87 cells maintained under standard adherent culture conditions, was upregulated in U87-NS cells, and decreased in the U87-FD cells (Figure 1*C*). Conversely, expression of the mature neuronal marker βIII-tubulin, which is low in hNSCs, was also low in U87 cells and U87-NS cells but upregulated in U87-FD cells (Figure 1*C*). We examined the expression levels of various other stem cell and reprogramming markers. Expression levels of CD133, Nanog, and Oct4 were found to be low in the U87 cells, upregulated in U87-NS cells, and downregulated in U87-FD cells (Figure 1, *D*–*F*). The capacity of the xenograft-derived

U87 cells to 1) self-renew as spheres in neural stem cell medium, 2) differentiate along multiple neural lineages, and 3) upregulate multiple markers and transcription factors associated with neural stem cells and GBM stem cells provides rigorous *in vitro* evidence for their stem-like phenotype.

U87-NS cells were found to have a functioning c-Met signaling cascade as evidenced by the phosphorylation of c-Met, AKT, and MAPK in response to purified recombinant HGF (Figure 1*G*). Treating U87-NS cells with the c-Met kinase inhibitor PF2341066 (150–300 nM) inhibited their capacity to form spheres consistent with a role for c-Met signaling in maintaining GBM stem-like cell self-renewal capacity *in vitro* as previously shown by us in other human GBM stem cell isolates (Figure 1*H*) [15]. Thus, U87 xenografts contain a subset of stem-like cells with a functional endogenously c-Met signaling cascade.

To test the hypothesis that therapeutic stem-like cell subpopulations within GBM are sensitive to *in vivo* c-Met pathway inhibition, we evaluated the effects of treating pre-established U87 xenografts with the neutralizing anti-HGF mAb L2G7 [5 mg/kg, every other

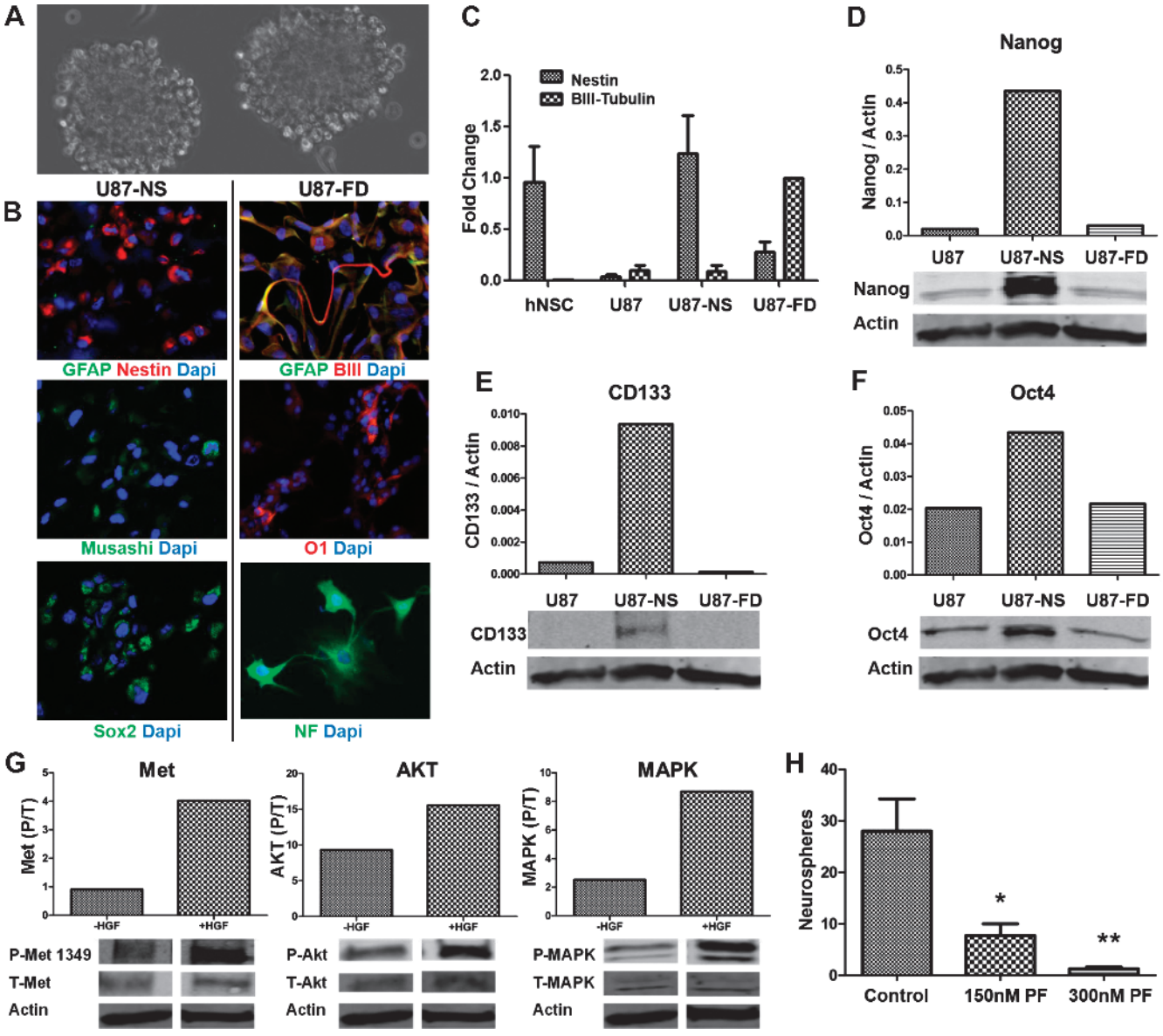

Figure 1. U87 xenografts contain multipotent neoplastic stem-like cells. (A) Xenograft-derived U87 cells form neurospheres (U87-NS, neurospheres) in serum-free stem neurosphere medium containing EGF and FGF. (B) Undifferentiated U87-NS cells express neural progenitor and stem cell markers GFAP (green), Nestin (red), Musashi (green), and Sox2 (green) (left panel). U87-NS cells subjected to conditions of forced differentiation (U87-FD) extend processes and exhibit morphologies consistent with neuronal lineage differentiation and express mature cell markers GFAP (green), βIII-tubulin (red), O1 (red), and neurofilament medium (NF) (green) (right panel). Nuclear counterstain DAPI is shown in blue. (C) Nestin and βIII-tubulin expression normalized to 18S RNA in hNSCs, U87, U87-NS, and U87-FD cells as determined by quantitative reverse transcription–polymerase chain reaction. (D–F) Immunoblot analysis of U87, U87-NS, and U87-FD cells showing expression of stem cell markers Nanog, CD133, and Oct4. (G) U87-NS cells stimulated with HGF for 30 minutes display increased phospho-Met tyr-1349, phospho-AKT, and phospho-MAPK. (H) Neurosphere formation by U87-NS cells is significantly inhibited by PF2341066. *$P < .05$, **$P < .001$, as compared with controls.

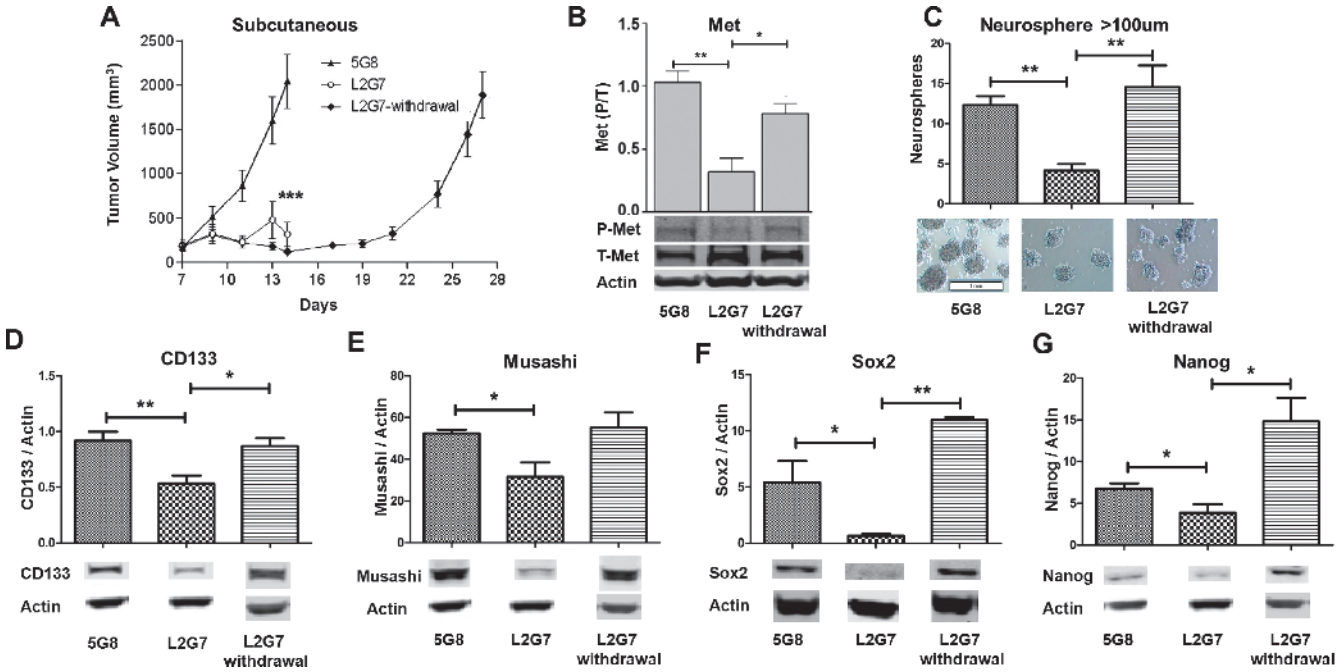

Figure 2. Systemic anti-HGF therapy inhibits tumor growth and modulates the stem-like phenotype in U87 xenografts. (A) Growth of subcutaneous tumor xenografts established from U87 cells and treated i.p. from PID 7 to 13 with control 5G8 mAb or with anti-HGF L2G7. L2G7 withdrawal depicts tumors treated with L2G7 for PID 7 to 13 followed by no therapy for PID 14 to 27 ($N = 6$). (B) Immunoblot analysis of tumor phospho–(tyr-1349)– and total Met levels in PID 14 U87 xenografts treated with 5G8 mAb or with L2G7 from PID 7 to 13 or in xenografts isolated on PID 27, 14 days after withdrawing L2G7 treatment ($N = 4$). (C) Neurosphere formation by cells derived from subcutaneous xenografts treated with 5G8 and L2G7 for PID 7 to 13 and following L2G7 withdrawal ($N = 6$). (D–G) Immunoblot analysis of tumor xenograft protein for CD133, Musashi, Sox2, and Nanog expression following L2G7 treatment and L2G7 withdrawal ($N = 4$). $^*P < .05$, $^{**}P < .001$, $^{***}P < .0001$ compared with control (5G8 treatment).

day, intraperitoneally (i.p.)] or with isotype mAb 5G8 as control under conditions previously shown to induce tumor regression [21]. L2G7 treatment resulted in a robust antitumor response ($P < .0001$; Figure 2*A*). Stopping L2G7 treatment in a subset of mice (referred to as L2G7 withdrawal, $N = 6$) resulted in tumor regrowth at a rate comparable to untreated controls (Figure 2*A*). The effects of L2G7 treatment on biologic and molecular markers of the stem-like cell phenotype were evaluated in tissues and cells obtained from post-implantation day (PID) 14 L2G7- and 5G8-treated xenografts and PID 28 xenografts 14 days after L2G7 withdrawal. L2G7 treatment inhibited tumor c-Met phosphorylation by ~69% ($P < .001$), concurrent with tumor growth arrest, as determined by immunoblot analysis of tumor protein (Figure 2*B*). Xenografts treated with L2G7 up to the time of sacrifice were depleted of sphere-forming stem-like cells ($P < .001$; Figure 2*C*). Expression of the stem cell markers CD133, Musashi, Sox2, and Nanog was statistically significantly lower in L2G7-treated xenografts (Figure 2, *D*–*G*). These results show that tumor stem-like cells are among the cell subpopulations targeted by c-Met pathway inhibition. The disproportionate loss of neurosphere-forming stem-like cells and the downregulated expression of stem cell markers and transcription factors in response to anti-HGF therapy are consistent with preferential targeting of stem-like cell subsets. Withdrawing L2G7 therapy resulted in a rebound in c-Met phosphorylation (Figure 2*B*), tumor sphere-forming capacity (Figure 2*C*), and tumor expression of molecular stem cell markers to magnitudes at least as high as those found in 5G8-treated controls (Figure 2, *D*–*G*). The transcription factors Sox2 and Nanog rebounded to levels approximately twice as high as those found in control tumors ($P < .001$ and $P < .05$, respectively; Figure 2, *F* and *G*). These results show that the neoplastic stem-like phenotype is dynamically regulated by the c-Met pathway activity *in vivo*.

Systemic c-Met Kinase Inhibitor Therapy Depletes HGF-Independent Human GBM Xenograft Lines of Stem-Like Cells

Glioma cells derived from the $HGF^-/c\text{-}Met^+$ Mayo 39 and Mayo 59 GBM xenograft lines express readily detectable levels of activated phospho–c-Met in the absence of HGF expression (Table W1). We used the small molecule c-Met kinase inhibitor PF2341066 to examine the effects of *in vivo* c-Met pathway inhibition on the stem-like phenotype in these HGF-independent glioma models. Subcutaneous xenografts were allowed to grow for approximately 23 days after which animals received PF2341066 (40 mg/kg daily by gavage) or carrier only as control for 7 days. PF2341066 statistically significantly inhibited the growth of both Mayo 59 ($P < .01$) and Mayo 39 ($P < .05$) xenografts (Figure 3*A*) concurrent with statistically significant inhibition of tumor c-Met activation by 50% to 80% as determined by immunoblot analysis of total tumor protein (Figure 3*B*). Similar to that observed in cells obtained from anti–HGF-treated U87 xenografts, systemic treatment with PF2341066 depleted xenografts of their stem-like sphere-forming cells (Figure 3, *C* and *D*). We examined the effects of systemic PF2341066 treatment on xenograft expression of stem cell–associated markers. Immunoblot analyses showed decreased expression of Nanog and Musashi in Mayo 59 xenografts and decreased expression of CD133 and Sox2 in Mayo 39 xenografts (Figure 3, *E* and *F*). These results show that *in vivo* c-Met inhibition

reduces tumor cell stemness in HGF-independent xenografts, similar to results in the HGF-dependent U87 xenograft model.

In Vivo *c-Met Pathway Inhibition Depletes Glioma Xenografts of Tumor-Propagating Cells*

Neurosphere-forming capacity and stem cell marker expression have been found to correlate with tumor-propagating potential in multiple solid tumor cell types including glioma. Therefore, our results presented above predict that c-Met pathway inhibition depletes tumor xenografts of tumor-propagating cells, one of the most clinically relevant neoplastic stem cell phenotypes. We asked if inhibiting c-Met signaling *in vivo* alters the capacity of tumor-derived cells to propagate orthotopic glioma xenografts (see Figure 4*A* for experimental schema). Pre-established subcutaneous U87 xenografts were treated with either anti-HGF L2G7 or control mAb 5G8 (5 mg/kg, i.p., every other day) for 1 week, the time at which c-Met was found to be inhibited by ~69% by anti-HGF (see Figure 2*B*). Tumors were dissected and single-cell suspensions of serially diluted tumor-derived cells (1×10^4, 3×10^3, or 3×10^2 viable cells per animal) were injected to the brain. This serial dilution tumor-propagating assay indirectly evaluates relative numbers of stem-like tumor-propagating cells within heterogeneous cell populations based on the efficiency of daughter xenograft formation. Animals in each group were sacrificed when the respective 5G8-treated control animals developed behavioral signs of impending death from tumor burden (i.e., PID day 19 for 1×10^4 cells/animal, PID 19 for 3×10^3 cells/animal, and PID 34 for 3×10^2 cells/animal). Histopathologic examination of H&E-stained brain sections revealed a reduction in tumor-propagating capacity by cells derived from anti–HGF-treated tumors (Figure 4*B*). In addition, the sizes of daughter xenografts that formed from anti–HGF-treated tumors were 12-fold smaller than controls (Figure 4*C*). Control animals consistently developed symptoms referable to tumor burden before controls reflecting the histopathologic findings. These results demonstrate that c-Met pathway inhibition depletes tumor xenografts of their most aggressive tumor-propagating stem-like cells.

Discussion

Therapies that target neoplastic stem-like cells offer promising new approaches for combating solid malignancies. Identifying and taking full advantage of stem cell–based cancer therapy requires a deeper understanding of the role for neoplastic stem-like cells in specific cancers and the molecular pathways driving the formation and tumor-propagating potential of neoplastic stem-like cells. We and others recently found

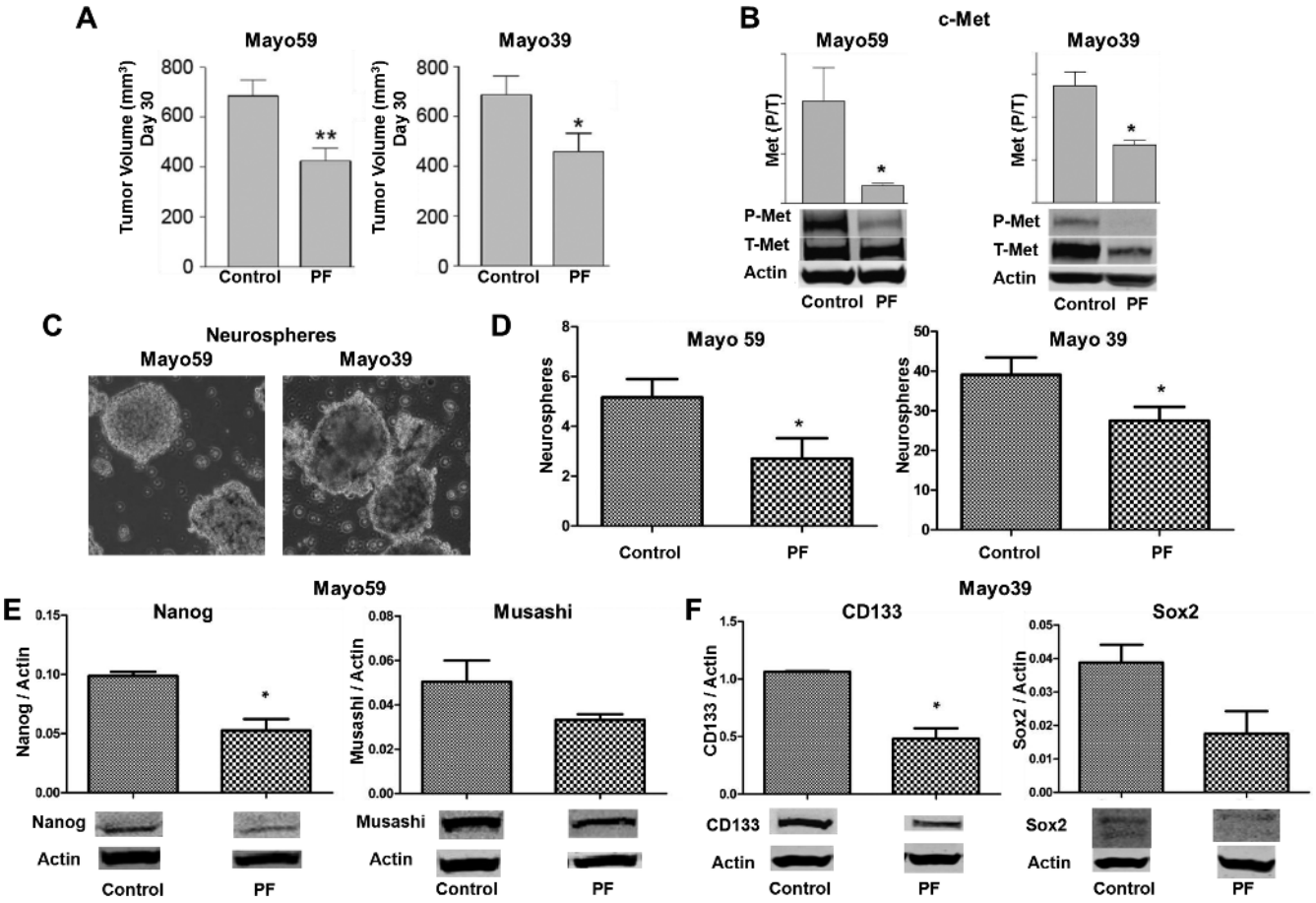

Figure 3. Systemic c-Met kinase inhibitor therapy inhibits tumor growth and depletes xenografts of stem-like cells. (A) Effects of PF2341066 (PF) on growth of Mayo 59 and Mayo 39 subcutaneous xenografts ($N = 5$). (B) Immunoblot analysis of phospho–(tyr-1349)– and total MET levels in control and PF-treated subcutaneous xenografts ($N = 4$). (C) Neurosphere formation by cells derived from control and PF-treated Mayo 59 and Mayo 39 xenografts. (D) Quantitation of neurosphere formation by cells derived from control and PF-treated xenografts ($N = 4$). (E) Immunoblot analysis of Nanog and Musashi expression levels in control and PF-treated Mayo 59 xenografts ($N = 4$). (F) Immunoblot analysis of CD133 and Sox2 expression in control and PF-treated Mayo 39 xenografts ($N = 4$). *$P < .05$, **$P < .001$.

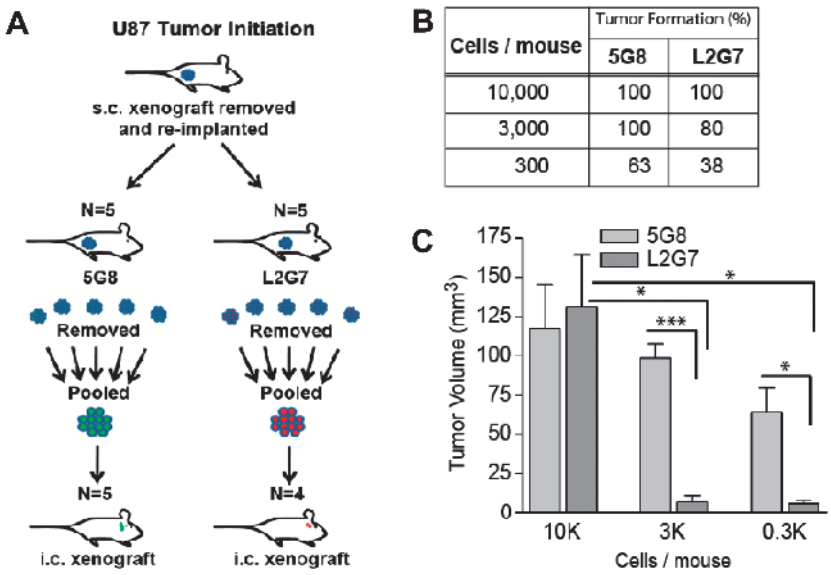

Figure 4. c-Met pathway inhibition depletes glioma xenografts of tumor-propagating cells. (A) Schematic of experimental design for testing the effect of anti-HGF (L2G7) therapy on the tumor-propagating capacity of U87 xenograft–derived cells. Animals bearing subcutaneous U87 xenografts were treated with 5G8 or L2G7 ($N = 5$). Tumors were recovered and tumor-derived cells were serially diluted and implanted intracranially using either 3×10^2 ($N = 8$), 3×10^3 ($N = 5$), and 1×10^4 ($N = 5$) viable cells/animal as shown. Animals were sacrificed and brains were assessed for daughter xenograft formation by analysis of H&E-stained histologic section. (B) The table shows the percentage of animals with detectable intracranial tumor xenografts. (C) Volumes of detectable tumors were quantified by computer-based image analysis as described in Materials and Methods section. *$P < .05$, **$P < .001$, ***$P < .0001$ compared with control (5G8 treatment).

that c-Met correlates with the stem-like phenotype in human glioblastoma cells and that c-Met signaling induces GBM cell stemness in *in vitro* model systems [13–15]. To determine if these previous findings have therapeutic implications, we asked if clinically translatable c-Met pathway inhibitors administered *in vivo* to glioblastoma-bearing animals target the pool of stem-like tumor-propagating cells. We investigated this question in three human glioblastoma xenograft models representing ligand-dependent and ligand-independent mechanisms of c-Met activation using two functionally distinct c-Met pathway inhibitors currently in clinical development. While the effects of c-Met pathway inhibitors are not limited to the tumor stem-like cell subpopulations, we show that inhibiting c-Met preferentially targets stem-like cells as evidenced by reductions in multiple molecular and biologic markers associated with cancer cell stemness and tumor-propagating potential. Numerous aspects of our experimental design and results make it unlikely that nonspecific antitumor effects (e.g., general cell "morbidity") explain the observed effects of c-Met pathway inhibition on tumor cell stemness. 1) We were very careful to input equal numbers of viable cells for all functional endpoints including *in vitro* neurosphere-forming capacity and *in vivo* tumor-propagating capacity. 2) Stem cell protein markers were quantified using methods rigorously normalized to housekeeping proteins and the results independently supported reduced stemness observed using biologic endpoints dependent on cell viability. These normalized biochemical endpoints would not be affected by nonspecific differences in the general state of the cell. 3) We observed that tumors regrow rapidly after withdrawing c-Met pathway inhibition, a behavior much more consistent with the reactivation of oncogenic RTK signaling and inconsistent with a general moribund state of the residual viable tumor cells. 4) c-Met inhibition also depleted the Mayo xenograft models of their stem-like cells even though there was less robust tumor growth inhibition in these models.

We and others have previously reported that neutralizing anti-HGF mAbs and c-Met kinase inhibitors can substantially inhibit the growth of glioblastoma xenografts derived from tumor cell lines consistent with the well-documented oncogenic effects of HGF/c-Met signaling in clinical and experimental glioblastoma [11,21,26]. We now present the novel findings that human glioblastoma xenograft lines, which express high levels of activated c-Met and more accurately replicate the histopathologic features of GBM, are also sensitive to c-Met inhibition. The different degrees of tumor growth inhibition achieved by anti-HGF mAb in U87 xenografts and PF2341066 in the Mayo xenograft lines are not likely to be due simply to different magnitudes of c-Met inhibition since we found that both agents similarly reduced tumor levels of phospho-Met in the current experiments. There are multiple potential reasons why the HGF-negative xenograft lines were found to be less sensitive than U87 xenografts to c-Met pathway inhibition. Xie et al. recently found that ligand-dependent c-Met activation predicts greater sensitivity to c-Met inhibitors than ligand-independent mechanisms of c-Met activation known to result from, for example, *c-met* gene amplification and RTK cross talk [27]. In addition, Mayo 39 and Mayo 59 cells express the constitutively activated EGF receptor (EGFR) deletion mutant EGFRvIII that supplies an alternate parallel pathway for oncogenic RTK signal hyperactivation and may drive cross-talk mechanisms leading to HGF-independent c-Met activation [20]. It is possible that simultaneously inhibiting EGFR and c-Met will be particularly affective against these xenograft lines as previously observed in U87 xenografts engineered to express EGFRvIII [21,28]. Experiments designed to answer this hypothesis are currently underway.

Our finding that c-Met pathway inhibitor therapy depletes three distinct xenograft models of multiple biologic and molecular markers of GBM cell stemness is consistent with a role for c-Met signaling in the generation and/or maintenance of GBM stem-like cells within

histologically complex tumors. This response after just 2 weeks of therapy and the relatively rapid rebound in tumor xenograft cell stemness after treatment withdrawal are consistent with the dynamic regulation of tumor cell stemness by c-Met signaling. These novel *in vivo* results mirror our recent *in vitro* findings showing that c-Met activation drives GBM cell stemness through reprogramming transcriptional mechanisms involving Sox2, Nanog, KLF4, and Oct-4 [15]. While our current findings focus on c-Met signaling, emerging evidence points to roles for other autocrine and paracrine signals derived from tumor cell subsets and the tumor microenvironment (e.g., macrophages and vascular cells) in maintaining neoplastic stem cell pools in solid tumors [4,29–33]. Strategies for assessing the relative contributions of these pathways to neoplastic cell stemness will be critical to the development of optimally effective stem cell–depleting personalized therapies in specific tumor subsets.

References

[1] Vescovi AL, Galli R, and Reynolds BA (2006). Brain tumour stem cells. *Nat Rev Cancer* **6**(6), 425–436.

[2] Bao S, Wu Q, McLendon RE, Hao Y, Shi Q, Hjelmeland AB, Dewhirst MW, Bigner DD, and Rich JN (2006). Glioma stem cells promote radioresistance by preferential activation of the DNA damage response. *Nature* **444**(7120), 756–760.

[3] Haar CP, Hebbar P, Wallace GC IV, Das A, Vandergrift WA III, Smith JA, Giglio P, Patel SJ, Ray SK, Banik NL, et al. (2012). Drug resistance in glioblastoma: a mini review. *Neurochem Res* **37**(6), 1192–1200.

[4] Heddleston JM, Li Z, McLendon RE, Hjelmeland AB, and Rich JN (2009). The hypoxic microenvironment maintains glioblastoma stem cells and promotes reprogramming towards a cancer stem cell phenotype. *Cell Cycle* **8**(20), 3274–3284.

[5] Seidel S, Garvalov BK, Wirta V, von Stechow L, Schanzer A, Meletis K, Wolter M, Sommerlad D, Henze AT, Nister M, et al. (2010). A hypoxic niche regulates glioblastoma stem cells through hypoxia inducible factor 2α. *Brain* **133**(pt 4), 983–995.

[6] Wang SD, Rath P, Lal B, Richard JP, Li Y, Goodwin CR, Laterra J, and Xia S (2012). EphB2 receptor controls proliferation/migration dichotomy of glioblastoma by interacting with focal adhesion kinase. *Oncogene* **31**, 5132–5143.

[7] Trusolino L, Bertotti A, and Comoglio PM (2010). MET signalling: principles and functions in development, organ regeneration and cancer. *Nat Rev Mol Cell Biol* **11**(12), 834–848.

[8] Abounader R and Laterra J (2005). Scatter factor/hepatocyte growth factor in brain tumor growth and angiogenesis. *Neuro Oncol* **7**(4), 436–451.

[9] Koochekpour S, Jeffers M, Rulong S, Taylor G, Klineberg E, Hudson EA, Resau JH, and Vande Woude GF (1997). Met and hepatocyte growth factor/scatter factor expression in human gliomas. *Cancer Res* **57**(23), 5391–5398.

[10] Li Y, Lal B, Kwon S, Fan X, Saldanha U, Reznik TE, Kuchner EB, Eberhart C, Laterra J, and Abounader R (2005). The scatter factor/hepatocyte growth factor: c-met pathway in human embryonal central nervous system tumor malignancy. *Cancer Res* **65**(20), 9355–9362.

[11] Kim KJ, Wang L, Su YC, Gillespie GY, Salhotra A, Lal B, and Laterra J (2006). Systemic anti-hepatocyte growth factor monoclonal antibody therapy induces the regression of intracranial glioma xenografts. *Clin Cancer Res* **12**(4), 1292–1298.

[12] Martens T, Schmidt NO, Eckerich C, Fillbrandt R, Merchant M, Schwall R, Westphal M, and Lamszus K (2006). A novel one-armed anti-c-Met antibody inhibits glioblastoma growth *in vivo*. *Clin Cancer Res* **12**(20 (pt 1)), 6144–6152.

[13] De Bacco F, Casanova E, Medico E, Pellegatta S, Orzan F, Albano R, Luraghi P, Reato G, D'Ambrosio A, Porrati P, et al. (2012). The MET oncogene is a functional marker of a glioblastoma stem cell subtype. *Cancer Res* **72**(17), 4537–4550.

[14] Joo KM, Jin J, Kim E, Ho Kim K, Kim Y, Gu Kang B, Kang YJ, Lathia JD, Cheong KH, Song PH, et al. (2012). MET signaling regulates glioblastoma stem cells. *Cancer Res* **72**(15), 3828–3838.

[15] Li Y, Li A, Glas M, Lal B, Ying M, Sang Y, Xia S, Trageser D, Guerrero-Cazares H, Eberhart CG, et al. (2011). c-Met signaling induces a reprogramming network and supports the glioblastoma stem-like phenotype. *Proc Natl Acad Sci USA* **108**(24), 9951–9956.

[16] Pandita A, Aldape KD, Zadeh G, Guha A, and James CD (2004). Contrasting *in vivo* and *in vitro* fates of glioblastoma cell subpopulations with amplified EGFR. *Genes Chromosomes Cancer* **39**(1), 29–36.

[17] Chaichana K, Zamora-Berridi G, Camara-Quintana J, and Quinones-Hinojosa A (2006). Neurosphere assays: growth factors and hormone differences in tumor and nontumor studies. *Stem Cells* **24**(12), 2851–2857.

[18] Ferrari D, Binda E, De Filippis L, and Vescovi AL (2010). Isolation of neural stem cells from neural tissues using the neurosphere technique. *Curr Protoc Stem Cell Biol* **Chapter 2**, Unit2D 6.

[19] Ying M, Sang Y, Li Y, Guerrero-Cazares H, Quinones-Hinojosa A, Vescovi AL, Eberhart CG, Xia S, and Laterra J (2011). Kruppel-like family of transcription factor 9, a differentiation-associated transcription factor, suppresses Notch1 signaling and inhibits glioblastoma-initiating stem cells. *Stem Cells* **29**(1), 20–31.

[20] Carlson BL, Pokorny JL, Schroeder MA, and Sarkaria JN (2011). Establishment, maintenance and *in vitro* and *in vivo* applications of primary human glioblastoma multiforme (GBM) xenograft models for translational biology studies and drug discovery. *Curr Protoc Pharmacol* **Chapter 14**, Unit 14 16.

[21] Lal B, Goodwin CR, Sang Y, Foss CA, Cornet K, Muzamil S, Pomper MG, Kim J, and Laterra J (2009). EGFRvIII and c-Met pathway inhibitors synergize against PTEN-null/EGFRvIII$^+$ glioblastoma xenografts. *Mol Cancer Ther* **8**(7), 1751–1760.

[22] Lal B, Xia S, Abounader R, and Laterra J (2005). Targeting the c-Met pathway potentiates glioblastoma responses to γ-radiation. *Clin Cancer Res* **11**(12), 4479–4486.

[23] Bleau AM, Howard BM, Taylor LA, Gursel D, Greenfield JP, Lim Tung HY, Holland EC, and Boockvar JA (2008). New strategy for the analysis of phenotypic marker antigens in brain tumor-derived neurospheres in mice and humans. *Neurosurg Focus* **24**(3–4), E28.

[24] Galli R, Binda E, Orfanelli U, Cipelletti B, Gritti A, De Vitis S, Fiocco R, Foroni C, Dimeco F, and Vescovi A (2004). Isolation and characterization of tumorigenic, stem-like neural precursors from human glioblastoma. *Cancer Res* **64**(19), 7011–7021.

[25] Sun P, Xia S, Lal B, Eberhart CG, Quinones-Hinojosa A, Maciaczyk J, Matsui W, Dimeco F, Piccirillo SM, Vescovi AL, et al. (2009). DNER, an epigenetically modulated gene, regulates glioblastoma-derived neurosphere cell differentiation and tumor propagation. *Stem Cells* **27**(7), 1473–1486.

[26] Burgess T, Coxon A, Meyer S, Sun J, Rex K, Tsuruda T, Chen Q, Ho SY, Li L, Kaufman S, et al. (2006). Fully human monoclonal antibodies to hepatocyte growth factor with therapeutic potential against hepatocyte growth factor/c-Met-dependent human tumors. *Cancer Res* **66**(3), 1721–1729.

[27] Xie Q, Bradley R, Kang L, Koeman J, Ascierto ML, Worschech A, De Giorgi V, Wang E, Kefene L, Su Y, et al. (2012). Hepatocyte growth factor (HGF) autocrine activation predicts sensitivity to MET inhibition in glioblastoma. *Proc Natl Acad Sci USA* **109**(2), 570–575.

[28] Pillay V, Allaf L, Wilding AL, Donoghue JF, Court NW, Greenall SA, Scott AM, and Johns TG (2009). The plasticity of oncogene addiction: implications for targeted therapies directed to receptor tyrosine kinases. *Neoplasia* **11**(5), 448–458, 2 p following 458.

[29] Li Y and Laterra J (2012). Cancer stem cells: distinct entities or dynamically regulated phenotypes? *Cancer Res* **72**(3), 576–580.

[30] Charles N, Ozawa T, Squatrito M, Bleau AM, Brennan CW, Hambardzumyan D, and Holland EC (2010). Perivascular nitric oxide activates notch signaling and promotes stem-like character in PDGF-induced glioma cells. *Cell Stem Cell* **6**(2), 141–152.

[31] Ikushima H, Todo T, Ino Y, Takahashi M, Miyazawa K, and Miyazono K (2009). Autocrine TGF-β signaling maintains tumorigenicity of glioma-initiating cells through Sry-related HMG-box factors. *Cell Stem Cell* **5**(5), 504–514.

[32] Jinushi M, Chiba S, Yoshiyama H, Masutomi K, Kinoshita I, Dosaka-Akita H, Yagita H, Takaoka A, and Tahara H (2011). Tumor-associated macrophages regulate tumorigenicity and anticancer drug responses of cancer stem/initiating cells. *Proc Natl Acad Sci USA* **108**(30), 12425–12430.

[33] Lathia JD, Gallagher J, Heddleston JM, Wang J, Eyler CE, Macswords J, Wu Q, Vasanji A, McLendon RE, Hjelmeland AB, et al. (2010). Integrin alpha 6 regulates glioblastoma stem cells. *Cell Stem Cell* **6**(5), 421–432.

Table W1. HGF Concentration in the Cells.

Cell Line	HGF (pg/μg)
U87wt	14.18
Mayo 39	0.00
Mayo 59	0.00

U87wt, Mayo 39, and Mayo 59 cells were grown under serum starvation conditions for 24 hours and then cells were washed with cold PBS three times. Proteins were extracted using RIPA buffer containing protease and phosphate inhibitors (Calbiochem) at 4°C and proteins were quantified using Coomassie Protein Assay (Pierce Thermo Scientific, Rockford, IL). HGF was quantified by using ELISA Kit (R&D Systems, Minneapolis, MN).